

DOI: 10.1070/QEL15826

Highly efficient, versatile, self-*Q*-switched, high-repetition-rate microchip laser generating Ince–Gaussian modes for optical trapping

Jun Dong, Yu He, Xiao Zhou, Shengchuang Bai

Abstract. **Lasers operating in the Ince-Gaussian (IG) mode have potential applications for optical manipulation of microparticles and formation of optical vortices, as well as for optical trapping and optical tweezers. Versatile, self-*Q*-switched, high-peak-power, high-repetition-rate Cr, Nd : YAG microchip lasers operating in the IG mode are implemented under tilted, tightly focused laser-diode pumping. An average output power of over 2 W is obtained at an absorbed pump power of 6.4 W. The highest optical-to-optical efficiency of 33.2% is achieved at an absorbed pump power of 3.9 W. Laser pulses with a pulse energy of 7.5 μJ, pulse width of 3.5 ns and peak power of over 2 kW are obtained. A repetition rate up to 335 kHz is reached at an absorbed pump power of 5.8 W. Highly efficient, versatile, IG-mode lasers with a high repetition rate and a high peak power ensure a better flexibility in particle manipulation and optical trapping.**

Keywords: *Ince–Guassian modes; Cr, Nd : YAG microchip lasers; laser-diode pumping, self-Q switching.*

1. Introduction

Lasers operating in the Ince–Guassian (IG) mode are of great interest because they combine all favorite properties of Laguerre–Gaussian and Hermite–Gaussian beams in a more general family where the ellipticity is used as an additional parameter in the elliptical coordinates [1, 2]. Potentials of IG beams have been demonstrated for such applications as optical manipulation of microparticles [3], formation of various optical vortices, optical trapping and optical tweezers [4]. IG beams have an elliptical intensity distribution combined with multiple phase singularities aligned on one axis, which might predestine them for investigations of the spatial behaviour of phase singularities [5, 6].

Spatial light modulators (SLMs) are widely used for generating IG beams [7]. A digital laser comprising an electrically addressed reflective phase-only SLM as an intra-cavity digitally addressed holographic mirror was demonstrated for selection of on-demand laser modes [8]. Various laser modes such as Laguerre–Gaussian, Hermite–Gaussian, flat-top and Airy modes were generated. However, the output power was only 12.5 mW at an absorbed pump power of 23.5 W, the optical efficiency being less than 0.1%. The low damage threshold of the SLM fabricated with liquid crystals limits the output power of the laser, including implementation of pulsed laser operation. In addition, the low resolution of the SLM cannot fully satisfy the requirements for desirable laser modes.

Fortunately, IG beams have been generated in diode-pumped solid-state lasers by breaking the resonator symmetry [9, 10]. However, these lasers exhibit continuous-wave operation, and their output power and efficiency are low due to the misalignment of the resonator. High-peak-power, high-repetition-rate pulsed lasers operating in the IG mode are a convenient tool for manipulating microparticles and increasing the resolutions of optical trapping and capacity of quantum computation. Self-*Q*-switched Cr, Nd : YAG microchip lasers with a nanosecond pulse width and over 1 kW peak power have been demonstrated to generate higher-order IG modes by applying a tilted pump beam [11]. Complicated transverse patterns have been generated in Cr, Nd : YAG microchip lasers by adjusting the pump beam diameter inside the Cr, Nd : YAG crystal [12]. The formation of IG modes and efficiency of the Cr, Nd : YAG microchip laser strongly depend on the pump power intensity, which is controlled by the applied pump power and the pump beam area. Therefore, the investigation of influence of the pump power intensity on the efficiency of a self-*Q*-switched Cr, Nd : YAG microchip laser operating in the IG mode is of undoubted interest.

In this paper, we report a highly efficient self-*Q*-switched Cr, Nd : YAG microchip laser operating in the IG mode under tightly focused laser-diode pumping. In addition, the parameters of the laser in question are presented.

2. Experimental setup

Figure 1 shows the schematic of a double-pass diode-end-pumped self-*Q*-switched Cr, Nd : YAG microchip laser operating in the IG mode, ensuring a specified pump power distribution inside the Cr, Nd : YAG crystal. A 1.8-mm-thick Cr, Nd : YAG crystal grown along the [111] direction was used as a gain medium of the laser. The doping concentrations of Cr and Nd ions were 0.01 at.% and 1 at.%, respectively. The initial transmission of the Cr, Nd : YAG crystal was 94%. An antireflection coating at 808 nm and a high reflection coating at 1064 nm were deposited on one surface of the crystal to act as a rear mirror of the laser cavity. An antireflection coating at 1064 nm and a high reflection coating at 808 nm were deposited on the other surface of the crystal to reduce the intra-cavity loss and to increase the absorption efficiency of the pump power, respectively. The output

Jun Dong, Yu He, Xiao Zhou, Shengchuang Bai Department of Electronics Engineering, School of Information Science and Engineering, Xiamen University, Xiamen, 361005, China; e-mail: jdong@xmu.edu.cn

Received 2 April 2015; revision received 13 November 2015
Kvantovaya Elektronika **46** (3) 218–222 (2016)
Submitted in English

coupler was a plane-parallel mirror with a reflection of 90% at 1064 nm. An 808-nm fibre coupled laser-diode with a core diameter of 400 μm and numerical aperture of 0.22 was used as a pump source. Two lenses with focal lengths of $f_1 = 8$ mm and $f_2 = 11$ mm were used to collimate and focus the pump beam on the Cr, Nd : YAG crystal. The diameter of the pump beam incident on the crystal was measured to be 160 μm. Under the same incident pump power as that in Ref. [11], the pump power intensity was about 1.6 times higher.

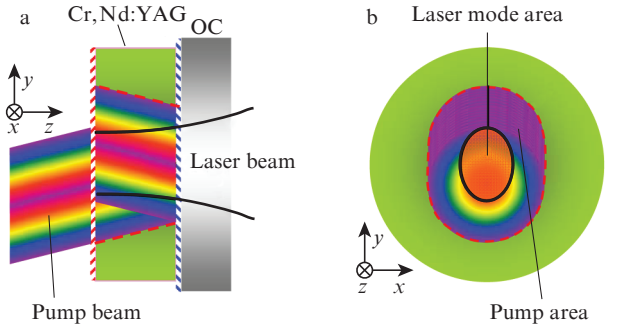

Figure 1. (a) Schematic of a self-Q-switched Cr, Nd : YAG microchip laser generating the IG mode, and (b) cross section of the pump power distribution and possible laser mode area; OC is the output coupler.

The incident pump beam after coupling optics was tilted by 3° away from the laser propagation direction (see Fig. 1a). The pump power distribution inside the Cr, Nd : YAG crystal was elliptical, i.e. the pump power intensity along the x axis is higher than that along the y axis. The elliptical distribution of the inversion population inside the Cr, Nd : YAG crystal broke the symmetry of the microchip laser cavity, and the nonlinear absorption of the Cr^{4+} saturable absorber enhanced the asymmetrical saturated inversion population distribution; therefore, the IG modes were forced to oscillate in the Cr, Nd : YAG microchip laser under a tilted pump beam. The output laser pulse characteristics were recorded with an InGaAs photodiode and 6-GHz oscilloscope. The laser spectra were monitored with an Anritus optical spectral analyser (MS9740A). The laser transverse distribution was controlled and recorded with a Thorlabs BC106-VIS CCD beam profiler.

3. Results and discussion

A tightly focused pump beam from a laser-diode, tilted away from the laser propagation direction, was used to force generation of IG modes in the Cr, Nd : YAG microchip lasers. However, the laser beam matched well with the pump beam because the plane-parallel Fabry–Perot cavity was used in the end-pumped Cr, Nd : YAG microchip lasers. The high pump power intensity was achieved when the pump beam diameter of 160 μm was applied in the experiment (unlike paper [11], where the pump beam diameter was 200 μm). One Cr^{4+} ion was surrounded by three thousand Nd^{3+} ions in the Cr, Nd : YAG crystal in question; therefore, the nonlinear absorption of the Cr^{4+} ions plays an important role in the IG mode oscillation.

When a Gaussian pump beam incident on the Cr, Nd : YAG crystal is tilted by 3° away from the laser propagation direction, the pump power distribution inside the double-pass Cr, Nd : YAG crystal is elliptical (Fig. 1b). Not all the pump area under laser-diode pumping has a sufficient gain to overcome the cavity loss for laser oscillation. The possible IG laser mode oscillation area strongly depends on the incident pump power (Fig. 2). When the pump power is low, the laser oscillates in a small elliptical laser mode area at the centre of the pump area (Fig. 2a) at an absorbed pump power $P_{abs} = 1$ W. The elliptical laser mode area increases asymmetrically within the pump area when the pump power is further increased. The pump power intensity increases along the x axis faster than along the y axis with the incident pump power (Fig. 2b; $P_{abs} =$ 3 W). At $P_{abs} = 6$ W, the laser mode area tends to be circular (Fig. 2c).

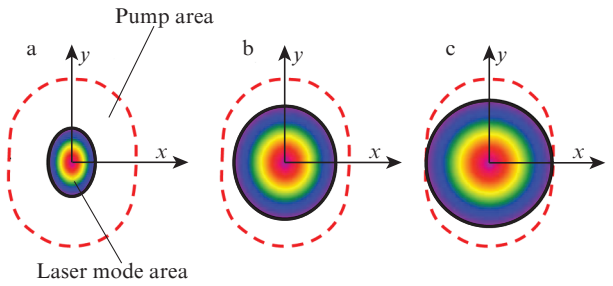

Figure 2. Dependence of the possible laser mode area on the absorbed pump power: P_{abs}= (a) 1, (b) 3 and (c) 6 W.

At $P_{abs} = 0.8$ W, the Cr, Nd : YAG microchip laser started to oscillate IG modes. Under tilted laser-diode pumping the oscillation of IG modes strongly depended on the inversion population distribution. Various odd ($IG^{o}_{p,m}$) and even ($IG^{e}_{p,m}$) IG modes were obtained by adjusting the pump power incident on the Cr, Nd : YAG crystal. All the IG mode laser beams generated in the Cr, Nd : YAG microchip laser exhibited the point symmetric transverse distribution. Figure 3 shows the typical single IG mode transverse field distribution observed experimentally in the self-Q-switched microchip Cr, Nd : YAG laser at $P_{abs} < 4$ W, together with the numerical simulation results by using IG mode expressions [2]. The transition from one IG mode oscillation to another was found to be sudden and abrupt with slowly and gradually increasing pump power incident on the Cr, Nd : YAG crystal. The odd IG mode and even IG mode oscillation in the Cr, Nd : YAG microchip laser was observed, depending on the applied pump power. A stable odd $IG^{o}_{1,1}$ mode was observed at $P_{abs} = 0.83$ W. When the pump power was above the laser threshold, the laser mode oscillated on a small part of the pump beam where the inversion population exceeded the losses of the Cr, Nd : YAG laser cavity, the laser mode area being elliptical which was determined by the tilted pump beam. Because the laser mode area extended faster along the x axis than along the y axis with the absorbed pump power, the ellipticity of the laser mode was decreased. The number of hyperbolic nodal lines, m, and the number of the elliptic nodal lines, $(p - m)/2$, increase with increasing P_{abs}. At $P_{abs} < 4$ W, various stable odd high-order IG modes ($IG^{o}_{4,4}$ and $IG^{o}_{8,4}$) and even high-order IG mode ($IG^{e}_{5,3}$, $IG^{e}_{6,4}$ and $IG^{e}_{7,5}$) modes were obtained depending on the pump power levels.

At $P_{abs} > 4$ W, the second IG mode starts to oscillate because the gain accumulated at the edge of the pump area is high enough to overcome the threshold of the second IG

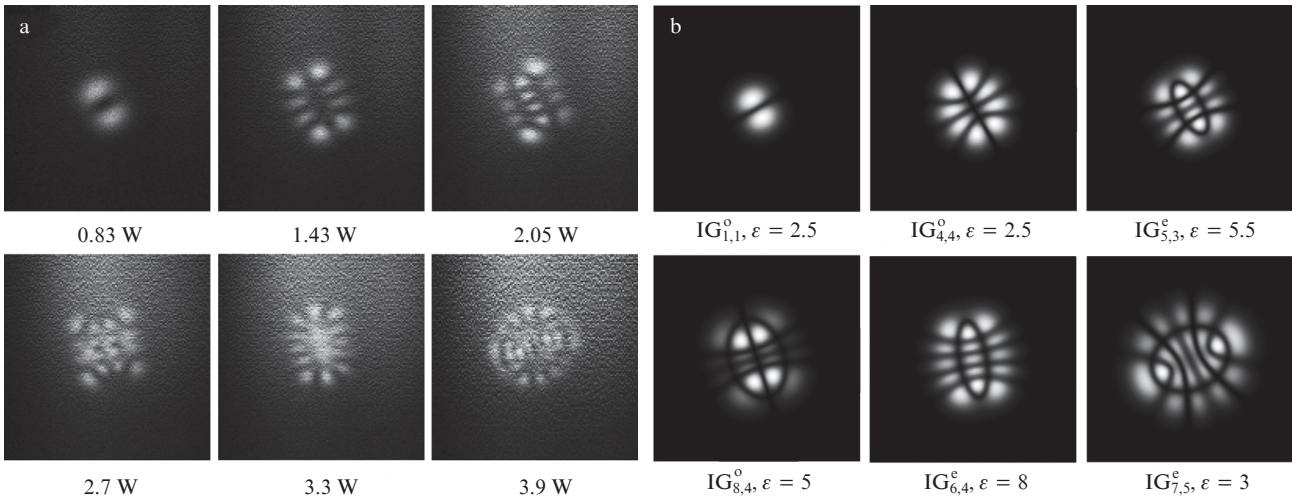

Figure 3. (a) Experimentally obtained single IG modes generated in the self-Q-switched Cr, Nd : YAG microchip laser at different pump power levels P_{abs}, and (b) corresponding theoretical simulation results; ε is the parameter of ellipticity.

mode. Meanwhile, two IG modes compete with each other. Due to this competition for the gain provided by the elliptical pump volume and gain saturation at a high pump power, the inversion population distribution tends to extend to the periphery of the pump area and the laser mode becomes circular. Therefore, the intensities of two IG laser modes nearly keep the same. Figure 4 shows two typical sets of IG modes oscillating simultaneously in the Cr, Nd : YAG microchip laser at $P_{abs} > 4$ W, together with the corresponding numerical simulation results. Two odd IG modes ($IG^{o}_{15,15}$ and $IG^{o}_{3,3}$) oscillate simultaneously at an absorbed pump power of 4.6 W. Two even IG modes ($IG^{e}_{15,13}$ and $IG^{e}_{3,3}$) start to simultaneously oscillate at $P_{abs} = 5.2$ W. With increasing P_{abs} to 5.8 W, they are replaced by two even IG modes ($IG^{e}_{13,7}$ and $IG^{e}_{19,19}$). The distribution of IG modes is affected by the thermal effect induced at high pump power levels. At $P_{abs} = 6.4$ W two even IG modes change to $IG^{e}_{9,5}$ and $IG^{e}_{17,17}$. The exchange of even IG modes with increasing absorbed pump power is caused by the variation of the pump power distribution with the absorbed pump power and the intracavity laser intensity induced gain guiding effect. The replacement of two even IG modes with P_{abs} clearly demonstrates strong competition for the gain between these IG modes in the Cr, Nd : YAG microchip laser.

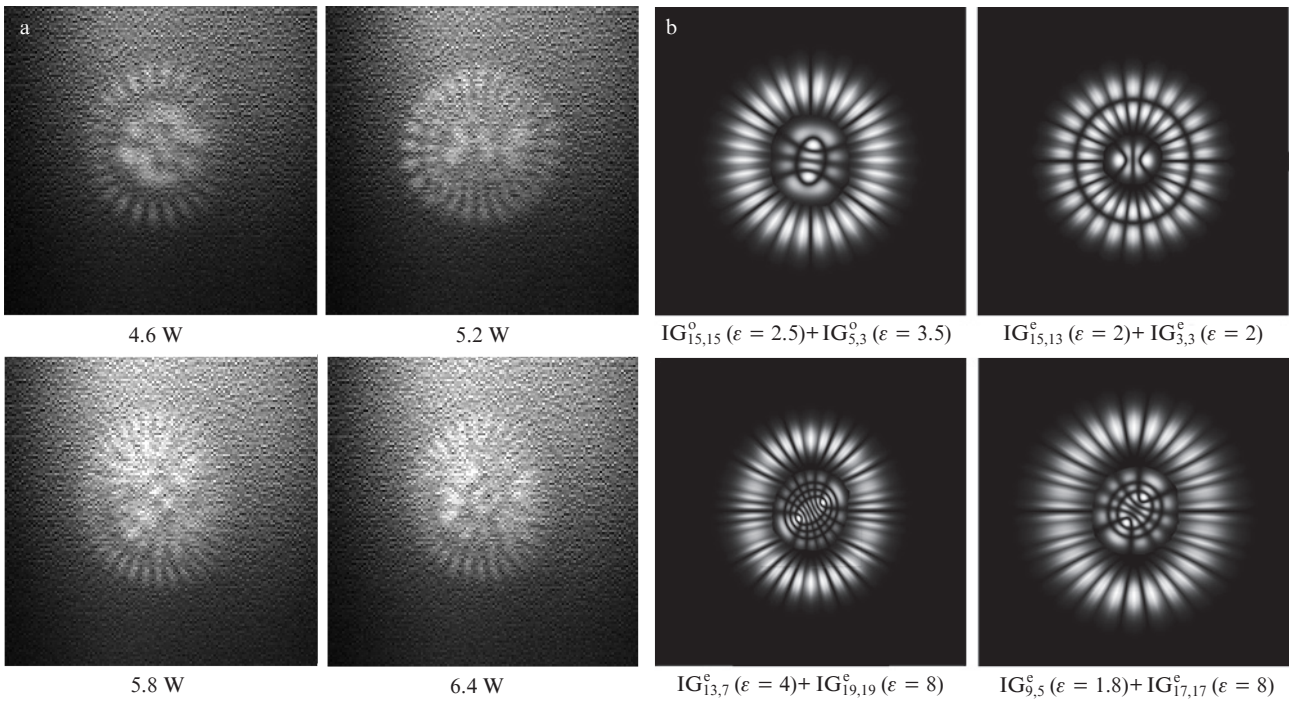

Figure 4. (a) Two experimentally obtained sets of IG modes generated in the self-Q-switched Cr, Nd : YAG microchip laser at different pump power levels P_{abs}, and (b) corresponding theoretical simulation results.

Figure 5 shows the variation of the average output power and optical-to-optical efficiency of the microchip laser as a function of P_{abs}. One can see that the average output power increases linearly with increasing absorbed pump power. However, there are two regions for variation of the average output power with the absorbed pump power. At $P_{abs} < 4$ W the slope efficiency is 45%, and at higher powers it drops down to 29%. The maximum average output power of 2.01 W was achieved at $P_{abs} = 6.4$ W and optical-to-optical efficiency of 31.3%. No rollover of the average output power was observed in the whole available pump power region; therefore, the average output power can be further scaled at higher pump powers. The maximum optical-to-optical efficiency of 33.2% was achieved at $P_{abs} = 3.9$ W, which is about 1.33 times higher than that obtained at a 200 μm pump beam diameter [11]. At $P_{abs} > 4$ W the optical-to-optical efficiency decreases slightly and then tends to keep constant with the absorbed pump power. The competition of two IG laser modes for the gain provided by the pump power is one reason for the optical-to-optical efficiency degradation when the absorbed pump power is higher than 4 W. The thermal effect is another factor affecting the optical-to-optical efficiency at a pump power higher than 4 W. Although the thermal loading of the Cr, Nd : YAG crystal degrades the laser performance at high pump power levels ($P_{abs} > 4$ W), the optical-to-optical efficiency of the laser under the tightly focused laser beam pumping keeps over 30% (as shown in Fig. 5). The efficient performance of the self-Q-switched Cr, Nd : YAG microchip laser shows that in the case of tightly focused laser-diode pumping, the Cr, Nd : YAG microchip laser is a stable laser source of IG modes, operating at room temperature even without active cooling of the laser head.

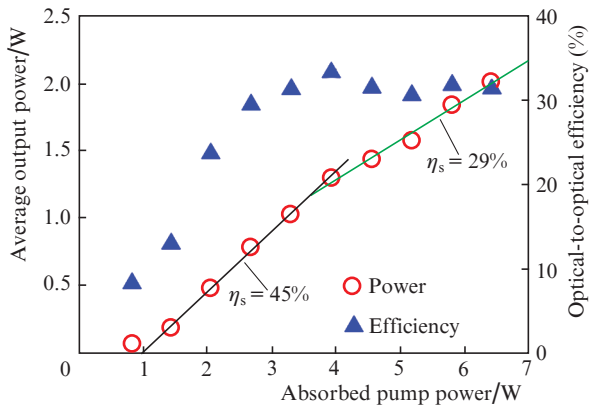

Figure 5. Average output power and optical-to-optical efficiency of the microchip laser generating IG modes vs. absorbed pump power; η_s is the slope efficiency.

The evolution of emission spectra of the microchip laser at different pump power levels is shown in Fig. 6. At $P_{abs} < 1.8$ W the laser oscillated in a single longitudinal mode. Although the emission bandwidth of Nd^{3+} ions in Cr, Nd : YAG is about 1 nm [13], the Cr, Nd : YAG microchip lasers oscillated in multi-longitudinal modes at high pump power levels because a 1.8-mm-thick Cr, Nd : YAG crystal was used as a gain medium. At $P_{abs} > 1.8$ W multi-longitudinal mode oscillation was dominant. The laser oscillated in two longitudinal modes when the absorbed pump power was in the range from 2 W to 3 W, and at $P_{abs} > 3$ W lasing occurred in three longitudinal modes. The longitudinal mode separation of the diode-pumped Cr, Nd : YAG microchip laser was 0.16 nm, which is determined by the free spectral range between the resonant modes (0.163 nm) in the laser cavity filled with the gain medium: $\Delta\lambda_c = \lambda^2/(2L_c)$ [14], where L_c is the optical length of the resonator and λ is the laser wavelength. The emission spectrum is broadened and shifts to the red with temperature [15, 16], which is raised with increasing pump power. The same behaviour is observed for the laser emitting wavelength.

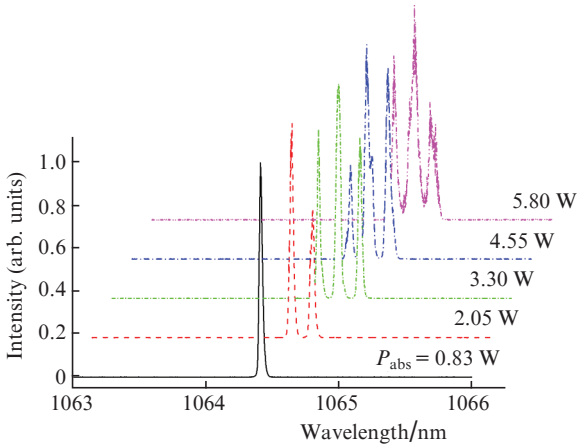

Figure 6. Evolution of emission spectra of the microchip laser operating in the IG mode with the variation of the absorbed pump power.

The repetition rate of the self-Q-switched Cr, Nd : YAG microchip laser increases virtually linearly with increasing absorbed pump power. The highest repetition rate up to 335 kHz was achieved at an absorbed pump power of 5.8 W. The repetition rate of passively Q-witched lasers is proportional to the inversion population provided by the pump power, which, in turn, is proportional to the pump power intensity. Therefore, the highest repetition rate was achieved when the smaller pump beam diameter was applied. The pulse width of the self-Q-switched Cr, Nd : YAG microchip laser was about 3.5 ns at any values of P_{abs}. The short pulse width may be caused by a high gain achieved at a high pump power intensity, which allows one to approach the round-trip pulse width limit more effectively [17]. Although the pulse energy of

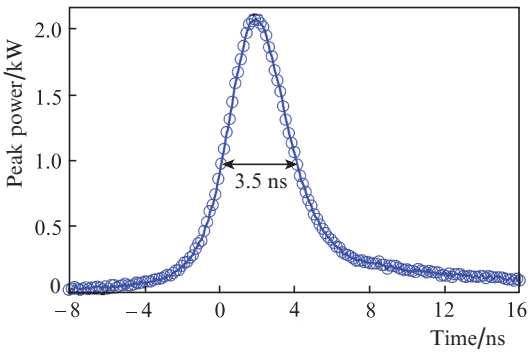

Figure 7. Typical pulse profile with a pulse width of 3.5 ns and peak power of over 2 kW at an absorbed pump power of 2.7 W.

7.5 μJ was limited by the small laser volume and high initial transmission of the Cr, Nd : YAG crystal, the peak power was kept comparable to that obtained in Ref. [11] owing to the short pulse width achieved at a high pump power intensity. The peak power obtained was 2.08 kW. Figure 7 shows a typical pulse profile of the microchip laser in question at P_{abs} = 2.7 W, pulse energy of 7.5 μJ, pulse width (FWHM) of 3.5 ns and pulse repetition rate of 108 kHz.

4. Conclusions

Highly efficient, high-repetition-rate and high-peak-power IG mode oscillation was achieved in a diode-pumped self-*Q*-switched Cr, Nd : YAG microchip laser by applying a tilted, tightly focused pump beam. The highest optical-to-optical efficiency of 33.2% was obtained at an absorbed pump power 3.9 W. A single IG-mode beam was produced at $P_{abs} < 4$ W and complicated beams consisting of two IG modes were observed at $P_{abs} > 4$ W. An average output power over 2 W was obtained at $P_{abs} = 6.4$ W. The highest repetition rate of laser pulses was equal to 335 kHz and depended on the pump power level. IG-mode laser pulses with a high repetition rate and a high peak power are promising for various applications such as manipulation of micro particles and optical trapping.

Acknowledgements. This work was supported by the National Natural Science Foundation of China (Grant Nos 61475130 and 61275143) and the Fundamental Research Funds for the Xiamen University (Project No. 201312G008).

References

1. Bandres M.A., Gutierrez-Vega J.C. *Opt. Lett.*, **29** (2), 144 (2004).
2. Bandres M.A., Gutierrez-Vega J.C. *J. Opt. Soc. Am. A*, **21** (5), 873 (2004).
3. Woerdemann M., Alpmann C., Denz C. *Appl. Phys. Lett.*, **98** (11), 111101 (2011).
4. Chu S.C., Yang C.S., Otsuka K. *Opt. Express*, **16** (24), 19934 (2008).
5. Woerdemann M., Alpmann C., Esseling M., Denz C. *Laser Photon. Rev.*, **7** (6), 839 (2013).
6. Plick W.N., Krenn M., Fickler R., Ramelow S., Zeilinger A. *Phys. Rev. A*, **87** (3), 033806 (2013).
7. Bentley J.B., Davis J.A., Bandres M.A., Gutierrez-Vega J.C. *Opt. Lett.*, **31** (5), 649 (2006).
8. Ngcobo S., Litvin I., Burger L., Forbes A. *Nature Commun.*, **4** (8), 2289 (2013).
9. Schwarz U.T., Bandres M.A., Gutierrez-Vega J.C. *Opt. Lett.*, **29** (16), 1870 (2004).
10. Ohtomo T., Kamikariya K., Otsuka K., Chu S.C. *Opt. Express*, **15** (17), 10705 (2007).
11. Dong J., Ma J., Ren Y.Y., Xu G.Z., Kaminskii A.A. *Laser Phys. Lett.*, **10** (8), 085803 (2013).
12. Dong J., Ueda K. *Phys. Rev. A*, **73** (5), 053824 (2006).
13. Dong J., Lu J., Ueda K. *J. Opt. Soc. Am. B*, **21** (12), 2130 (2004).
14. Koechner W. *Solid State Laser Engineering* (Berlin: Springer-Verlag, 1999).
15. Dong J., Rapaport A., Bass M., Szipocs F., Ueda K. *Phys. Status Solidi (a)*, **202** (13), 2565 (2005).
16. Rapaport A., Zhao S.Z., Xiao G.H., Howard A., Bass M. *Appl. Opt.*, **41** (33), 7052 (2002).
17. Agnesi A., Pirzio P., Reali G., Piccinno G. *Appl. Phys. Lett.*, **89** (10), 101120 (2006).